Available online at www.sciencedirect.com
ScienceDirect
Journal of Membrane Science 284 (2006) 237–247
journal of MEMBRANE SCIENCE
www.elsevier.com/locate/memsci

Influence of concentrative and dilutive internal concentration polarization on flux behavior in forward osmosis

Jeffrey R. McCutcheon, Menachem Elimelech *

Department of Chemical Engineering, Environmental Engineering Program, Yale University, P.O. Box 208286, New Haven, CT 06520-8286, USA

Received 23 May 2006; received in revised form 21 July 2006; accepted 24 July 2006
Available online 11 August 2006

Abstract

Osmosis through asymmetric membranes has been studied as a means of desalination via forward osmosis and power generation through a process known as pressure retarded osmosis. The primary obstacle to using asymmetric membranes for osmotic processes is the presence of internal concentration polarization, which significantly reduces the available osmotic driving force. This study explores the impact of both concentrative and dilutive internal concentration polarization on permeate water flux through a commercially available forward osmosis membrane. The coupling of internal and external concentration polarization is also investigated. A flux model that accounts for the presence of both internal and external concentration polarization for the two possible membrane orientations involving the feed and draw solutions is presented. The model is verified by data obtained from laboratory-scale experiments under well controlled conditions in both membrane orientations. Furthermore, the model is used to predict flux performance after hypothetical improvements to the membrane or changes in system conditions.

Keywords: Forward osmosis; Pressure retarded osmosis; Desalination; Concentration polarization; Internal concentration polarization

1. Introduction

The separation of water from aqueous solutions using synthetic polymeric membranes has been studied intensely for the past half century. Over this time, pressure-driven membrane separations, namely microfiltration (MF), ultrafiltration (UF), nanofiltration (NF), and reverse osmosis (RO) have become more popular as a viable separation technique for removing undesired solutes from a solution. These pressure-driven membrane processes have been employed heavily in the field of water treatment, namely for filtration and desalination.

The major drawback of these pressure-driven membrane processes, especially in RO desalination, is their operating cost. Significant hydraulic pressures are required to overcome the osmotic pressures of the source waters. This not only requires significant energy, but also limits the feed water recovery and hence produces a concentrated brine discharge. Brine discharge has an environmental cost and limits the use of large-scale membrane desalination to coastal areas where the brine can be discharged out to sea. This critical environmental drawback, coupled with only incremental annual decreases in cost for RO processes, has led to investigation into alternate means of desalinating water.

Using forward osmosis (FO) as an alternative to pressure-driven membrane processes has been gaining some popularity in the last few years. Conceptually proposed three decades ago [1,2], FO uses a concentrated draw solution to generate an osmotic pressure gradient across a semi-permeable membrane. Water will naturally traverse the membrane via osmosis into the draw solution. The draw solute is then either ingested [3], discarded, or removed from the product water and recycled [4–7].

With many solutes being very effective osmotic agents (i.e., highly soluble and having a low molecular weight), the osmotic pressure gradients that can be generated are enormous compared to the hydraulic pressures used in RO. The prospect of naturally occurring osmotic pressure gradients even prompted the exploration of using FO as a means of power production when fresh river water mixes with sea water, via a process called pressure retarded osmosis (PRO) [8–12]. However, these studies in FO and PRO all came to the same conclusion: permeate water fluxes were far lower than anticipated based on the osmotic pressure

* Corresponding author. Tel.: +1 203 432 2789; fax: +1 203 432 2881.
E-mail address: menachem.elimelech@yale.edu (M. Elimelech).

0376-7388/$ – see front matter © 2006 Elsevier B.V. All rights reserved.
doi:10.1016/j.memsci.2006.07.049

difference across the membrane and the water permeability coefficient of the membrane.

The primary reason for this finding is mired in the fact that membrane development over the past four decades has occurred based on their use in pressure driven, rather than osmotically driven, processes. This has meant the designing of membranes with very thin (and therefore highly permeable) dense layers which reject the undesired solute, and very thick porous support layers which mechanically support this thin active layer under the hydraulic pressures required for operation [13].

In a pressure-driven membrane process, mass transfer on the permeate side of the membrane is unimportant. It is only important on the feed side of the membrane where concentration polarization effects [14,15] will reduce the permeate water flux and can induce scaling or fouling. In an osmotic process, however, mass transfer is critical on both sides of the membrane. On the feed side, the polarized layer is more concentrated than the bulk, as in RO, while on the permeate (draw) side, the layer is more dilute. The severity of these effects can be controlled to some degree with crossflow and well designed hydrodynamics. When the membrane used is asymmetric, however, one of these polarization effects is protected within the confines of a porous support layer where crossflow cannot mitigate it.

The objective of this paper is to systematically investigate this phenomenon, referred to as internal concentration polarization (ICP), and elucidate its effect on permeate water flux for a previously studied commercial FO membrane. Data from experiments utilizing this membrane in the two possible orientations involving the feed and draw solutions will be presented to describe dilutive and concentrative ICP, respectively. A model that combines both internal and external concentration polarization is used to verify the experimental water flux results at different temperatures using a well characterized solute (NaCl).

2. Materials and methods

2.1. Feed and draw solutions

The feed and draw solutions were both composed of NaCl. The feed solution concentration ranged from 0 (deionized water) to 1.0 M, whereas the draw solution ranged from 0.05 to 1.5 M. Solution characteristics, such as viscosity, density, and osmotic pressure were calculated using software from OLI Systems Inc. (Morris Plains, NJ) and Aspen HYSYS® (Cambridge, MA). NaCl was the only solute used since it is easily characterized for osmotic pressure and diffusion coefficient. Water flux was the only performance parameter studied. NaCl rejection performance of the FO process was previously reported for this membrane [6,7].

2.2. Forward osmosis membrane

The membrane used was provided by Hydration Technologies, Inc. (Albany, OR). This membrane has been used in our previous studies on FO [6,7]. The membrane chemistry is proprietary, though it is believed to consist of cellulose based polymers and is hence denoted CA in this paper. This commercially available FO membrane is designed to not require a thick fabric backing layer for mechanical support, unlike current generation RO membranes. A polymer porous support layer is present, however, giving the membrane asymmetry [6]. The membrane uses an embedded polyester mesh to provide additional mechanical stability normally provided by a fabric backing in RO membranes, thus allowing the overall membrane thickness to be much less than in RO. The total thickness of the CA membrane is less than 50 μm [6].

2.3. Forward osmosis crossflow system

The experimental crossflow FO system is similar to that described in our earlier studies [6,7], with slight modifications. The crossflow membrane unit is custom built with channels on both sides of the membrane. The dimensions of the channel are 77 mm long by 26 mm wide by 3 mm deep. Counter current crossflow is used. Mesh spacers were inserted within both channels to improve support of the membrane as well as to promote turbulence and mass transfer. Variable speed gear pumps (Micropump, Vancouver, WA) were used to pump the liquids in a closed loop. A constant temperature water bath (Neslab, Newington, NH) was used to maintain both the feed and draw solution temperature. Heat transfer took place within the water bath through inline stainless steel heat exchanger coils which were submerged in the bath. The draw solution rested on a scale (Denver Instruments, Denver, CO) and weight changes were measured over time to determine the permeate water flux.

2.4. Forward osmosis runs

Forward osmosis runs were conducted using both possible orientations of the asymmetric CA membrane. The first run oriented the draw solution against the active layer and the more dilute feed against the porous support layer. This orientation has been used in previous studies on PRO, as the porous support layer is required to resist the pressurization of the permeate stream [8,16], and will be referred to as the PRO mode. None of the runs in this study, however, used any hydraulic pressure on either side of the membrane. In the other orientation, the draw solution is placed against the support layer and the dilute feed is on the active layer. This is the typical orientation in FO, as was described in our previous studies on FO desalination [6,7], and will be referred to as the FO mode.

The following experimental protocol was used for both orientations. The system was first run with deionized water on both sides of the membrane to allow for temperature equilibration. Concentrated NaCl (5 M) stock solution was then added to the draw solution side to establish a draw solution of the desired concentration and the flux was measured. After the flux measurement was taken, more NaCl stock solution was added to the draw solution to achieve the next desired concentration. This procedure was followed for draw concentrations of 0.05, 0.1, 0.5, 1, and 1.5 M NaCl. These stepwise increases in draw solution concentration yielded flux as represented by the solid arrow in Fig. 1.

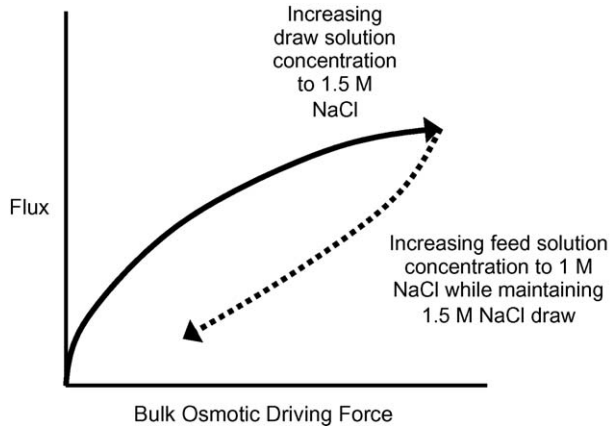

Fig. 1. Schematic diagram depicting the FO testing procedure. Using a deionized water feed, the draw solution is incrementally increased in concentration up to 1.5 M NaCl on one side of the membrane, represented by the solid line. A subsequent increase in NaCl feed solution concentration while using the 1.5 M NaCl draw solution produces the dashed line.

After a flux measurement was taken at the final concentration of 1.5 M NaCl draw solution with deionized water feed, 5 M NaCl stock solution was added in appropriate amounts to the feed side to establish a desired feed solution concentration. Flux was determined at feed concentrations of 0.05, 0.1, 0.5, and 1 M NaCl. Draw solution concentration was assumed constant at 1.5 M during this series of tests, since volumetric flux was low relative to the volume of the draw solution. This set of data is represented by the dotted line in Fig. 1.

It is important to note that volumetric changes in either solution due to water flux were taken into account when calculating the amount of 5 M NaCl stock solution to add to the draw and feed solution sides. The experimental protocol described above is advantageous for testing ICP effects since it does not require membrane replacement for each test and eliminates errors caused by variability between membranes.

3. Modeling flux and concentration polarization

Concentration polarization is a significant problem in pressure-driven membrane desalination processes and has thus been the target of several investigations [13–15]. Its presence inhibits permeate flow due to an increased osmotic pressure at the membrane active layer surface. In this study, we refer to this as external concentration polarization (ECP). In osmotic processes, concentration polarization can occur on both sides of the membrane. On the feed side, the solute is concentrated at the membrane surface. On the permeate side, the solute is diluted at the membrane surface. We refer to these two linked phenomena as concentrative and dilutive ECP, respectively.

When the membrane being used is asymmetric, one of these boundary layers occurs within the porous support layer of the membrane, protecting it from the shear and turbulence associated with crossflow along the membrane surface. We refer to this phenomenon as either concentrative or dilutive *internal* concentration polarization (ICP). Below, these four concentration polarization phenomena are quantitatively described.

3.1. Concentrative and dilutive external concentration polarization

Concentrative ECP refers to a well understood phenomenon that currently afflicts pressure-driven membrane processes. Convective water flow drags solute from the bulk solution to the surface of the rejecting active layer. Water permeates this layer leaving the solute behind in higher concentrations. The driving force must overcome this increased concentration in order for water flux to occur. Concentrative ECP also occurs in FO when the feed solution is placed against the active layer of the membrane.

Knowing the overall effective osmotic driving force is important in determining the flux performance in FO. We, therefore, need to determine the concentration of the feed at the active layer surface. This is not an easily measurable quantity, though it can be calculated from experimental data using boundary layer film theory. Determining the membrane surface concentration, outlined in McCutcheon et al. [7] and others [13,17], begins with the calculation of the Sherwood number for the appropriate flow regime in a rectangular channel:

$$Sh = 1.85\left(Re\,Sc\frac{d_h}{L}\right)^{0.33} \quad \text{(laminar flow)} \tag{1}$$

$$Sh = 0.04Re^{0.75}Sc^{0.33} \quad \text{(turbulent flow)} \tag{2}$$

Here, Re is the Reynolds number, Sc the Schmidt number, d_h is the hydraulic diameter, and L is the length of the channel. The mass transfer coefficient, k, is related to Sh by

$$k = \frac{Sh\,D}{d_h} \tag{3}$$

where D is the solute diffusion coefficient. The mass transfer coefficient is then used to calculate what is called the concentrative ECP modulus:

$$\frac{\pi_{F,m}}{\pi_{F,b}} = \exp\left(\frac{J_w}{k}\right) \tag{4}$$

where J_w is the experimental permeate water flux, and $\pi_{F,m}$ and $\pi_{F,b}$ are the osmotic pressures of the feed solution at the membrane surface and in the bulk, respectively. Note that the exponent is positive, indicating that $\pi_{F,m} > \pi_{F,b}$. Concentrative ECP only occurs on the feed side of a membrane. Furthermore, in this equation we assume that the ratio of the membrane surface concentration of feed solute to the bulk concentration is equal to the corresponding ratio of osmotic pressures. This is a reasonable assumption for relatively dilute solutions where osmotic pressure is proportional to salt concentration.

Dilutive ECP is a phenomenon similar to concentrative ECP, except that in this case, convective water flow is displacing and dragging the dissolved draw solute away from the membrane surface on the permeate side of the membrane. This reduces the effective driving force of the draw solution. A dilutive ECP modulus can be defined as above, except that in this case, the membrane surface concentration of the draw solute is less than

that of the bulk [7]:

$$\frac{\pi_{D,m}}{\pi_{D,b}} = \exp\left(-\frac{J_w}{k}\right) \quad (5)$$

Here, $\pi_{D,m}$ and $\pi_{D,b}$ are the osmotic pressures of the draw solution at the membrane surface and in the bulk, respectively. As with Eq. (4), it is assumed that the ratio of the membrane surface concentration of draw solute to the bulk concentration is equal to the corresponding ratio of osmotic pressures.

To model the flux performance of the FO process in the presence of ECP, we start with the standard flux equation for FO, given as

$$J_w = A(\pi_{D,b} - \pi_{F,b}) \quad (6)$$

where A is the pure water permeability coefficient. We assume that salt does not cross the membrane, or that σ, the osmotic reflection coefficient, has a value of 1. Eq. (6) predicts flux as a function of driving force only in the absence of concentrative or dilutive ECP, which may be valid only if the permeate flux is very low. When flux rates are higher, however, this equation must be modified to include both the concentrative and dilutive ECP:

$$J_w = A\left[\pi_{D,b}\exp\left(-\frac{J_w}{k}\right) - \pi_{F,b}\exp\left(\frac{J_w}{k}\right)\right] \quad (7)$$

A diagram depicting this phenomenon with a dense symmetric membrane is given in Fig. 2(a). However, no dense symmetric membranes are in use today for osmotic processes and therefore, the usefulness of this particular flux model is limited. We must therefore consider the case where the membrane is asymmetric, a case for which ICP effects are most significant.

3.2. Concentrative internal concentration polarization

When the feed is placed against the support layer of an asymmetric membrane (as in PRO applications), water enters the porous support layer and diffuses across the active layer into the draw solution. The salt in the feed freely enters the open structure as it is transported into this layer by convective water flow. The salt cannot easily penetrate the active layer from the support layer side and therefore increases in concentration within the porous layer. This is referred to as concentrative ICP [18].

Lee et al. [8] derived an expression modeling this phenomenon in PRO, which Loeb et al. [19] later described for osmosis. This expression describes ICP effects and how they relate to water flux and other membrane constants:

$$K = \left(\frac{1}{J_w}\right)\ln\frac{B + A\pi_{D,m} - J_w}{B + A\pi_{F,b}} \quad (8)$$

Here, B is the salt permeability coefficient of the active layer and K is the solute resistivity for diffusion within the porous support layer, defined by

$$K = \frac{t\tau}{D\varepsilon} \quad (9)$$

where D is the diffusion coefficient of the solute, and t, τ, and ε are the thickness, tortuosity, and porosity of the support layer, respectively. K is a measure of how easily a solute can diffuse

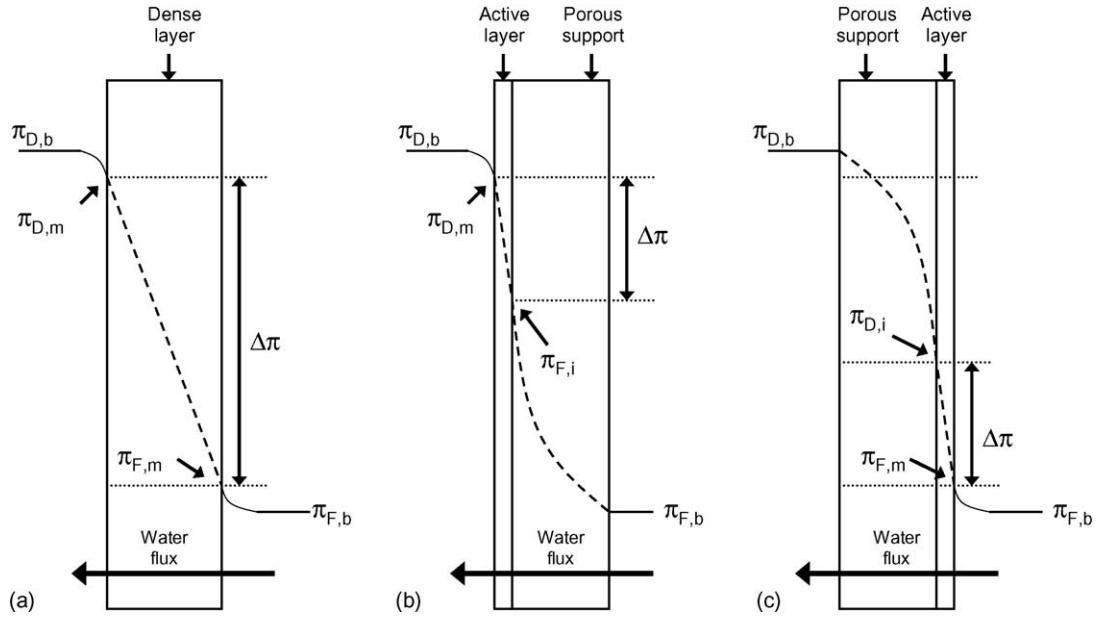

Fig. 2. Illustration of osmotic driving force profiles for osmosis through several membrane types and orientations, incorporating both internal and external concentration polarization. (a) A symmetric dense membrane; the profile illustrates concentrative and dilutive ECP. (b) An asymmetric membrane with the dense active layer against the draw solution (PRO mode); the profile illustrates concentrative ICP and dilutive ECP. (c) An asymmetric membrane with the porous support layer against the draw solution (FO mode); the profile illustrates dilutive ICP and concentrative ECP. Key: $\pi_{D,b}$ is the bulk draw osmotic pressure, $\pi_{D,m}$ is the membrane surface osmotic pressure on the permeate side, $\pi_{F,b}$ is the bulk feed osmotic pressure, $\pi_{F,m}$ is the membrane surface osmotic pressure on the feed side, $\pi_{F,i}$ is the effective osmotic pressure of the feed in PRO mode, $\pi_{D,i}$ is the effective osmotic pressure of the draw solution in FO mode, and $\Delta\pi$ is the effective osmotic driving force. Note that it is assumed that no ECP occurs along the porous support layer since NaCl is not reflected by the layer; in these cases, bulk osmotic pressure is equivalent to membrane surface osmotic pressure.

into and out of the support layer and thus is a measure of the severity of ICP.

For membranes which reject salt to a high degree and operate at high flux, B is negligible compared to the other terms in Eq. (8). Therefore, as mentioned earlier, we ignore salt flux in the direction of water flux and any passage of salt from the permeate (draw solution) side. Upon rearrangement, flux can be solved for implicitly from Eq. (8):

$$J_w = A[\pi_{D,m} - \pi_{F,b}\exp(J_w K)] \tag{10}$$

Eq. (10) defines water flux as a product of the water permeability coefficient and the effective osmotic driving force. The exponential term is a correction factor that can be considered the concentrative ICP modulus, defined as

$$\frac{\pi_{F,i}}{\pi_{F,b}} = \exp(J_w K) \tag{11}$$

where $\pi_{F,i}$ is the osmotic pressure of the feed solution on the inside of the active layer within the porous support. The positive exponent indicates that $\pi_{F,i} > \pi_{F,b}$, or that the effect is concentrative. Fig. 2(b) illustrates concentrative ICP. Note that it is assumed that no ECP occurs on the outer surface of the porous support because the salt is assumed to be completely permeable through this layer.

Eq. (10) requires the input of a membrane surface concentration on the permeate side of the membrane in order to predict flux. Since this value is not measurable, we can substitute Eq. (5) into (10) to obtain an analytical model for the effect of ICP and ECP on permeate flux, which includes only measurable quantities:

$$J_w = A\left[\pi_{D,b}\exp\left(-\frac{J_w}{k}\right) - \pi_{F,b}\exp(J_w K)\right] \tag{12}$$

All the terms in Eq. (12) are readily determined through experiments or calculations. By solving Eq. (12), we can predict the water flux through an asymmetric membrane where the feed is placed against the support layer and the draw solution against the active layer.

3.3. Dilutive internal concentration polarization

When the feed solution is against the active layer and the draw solution is against the backing layer, as in the case of FO desalination, the ICP phenomenon now occurs on the permeate side. We refer to this as dilutive ICP since the draw solution is diluted by the permeate water within the porous support of the membrane [18]. Dilutive ICP is illustrated in Fig. 2(c). Loeb et al. [19] similarly described flux behavior in the FO mode:

$$K = \left(\frac{1}{J_w}\right)\ln\frac{B + A\pi_{D,b}}{B + J_w + A\pi_{F,m}} \tag{13}$$

When assuming that the salt permeability is negligible (i.e., $B = 0$, $\sigma = 0$) and the equation is rearranged, an implicit equation for the permeate water flux is obtained:

$$J_w = A[\pi_{D,b}\exp(-J_w K) - \pi_{F,m}] \tag{14}$$

Here, $\pi_{D,b}$ is now corrected by the dilutive ICP modulus, given by

$$\frac{\pi_{D,i}}{\pi_{D,b}} = \exp(-J_w K) \tag{15}$$

where $\pi_{D,i}$ is the concentration of the draw solution on the inside of the active layer within the porous support. The negative exponent is indicative of dilution at this point, or $\pi_{D,i} < \pi_{D,b}$.

By substituting Eq. (4) into (14), we get

$$J_w = A\left[\pi_{D,b}\exp(-J_w K) - \pi_{F,b}\exp\left(\frac{J_w}{k}\right)\right] \tag{16}$$

which models water flux for an asymmetric membrane, where the draw solution is placed against the support layer and the feed against the active layer, as in FO desalination. Again, the terms in Eq. (16) are measurable system conditions and membrane parameters. Note that here, dilutive ICP is coupled with concentrative ECP, whereas in the previous section, Eq. (12), concentrative ICP was coupled with dilutive ECP.

In each of these cases, the ECP and ICP moduli all contribute negatively to the overall osmotic driving force. The negative contribution increases with increasing flux, which creates a situation where flux is self-limiting. This suggests that increasing bulk osmotic driving force will provide diminishing increases in flux. The experimental data below helps delineate the contribution of the ECP and ICP to the driving force. The models presented here are compared to these data later in the paper, requiring the calculation of the ECP and ICP moduli. The ECP modulus is easily calculable using known experimental conditions in conjunction with Eqs. (1)–(5). The ICP modulus, however, is more complicated to calculate due to the solute resistivity term, K. The latter is a function of membrane characteristics which are difficult to determine or often unavailable due to proprietary issues. We will revisit this subject later in Section 4.2.

4. Results and discussion

4.1. Flux behavior at different temperatures

Forward osmosis water flux data were collected at 20, 30, and 40 °C in order to determine the effect of temperature on water flux. It was hypothesized that increasing temperature would increase water flux in a manner similar to that of RO. Flux increases in RO with increasing temperature are primarily due to a decreased viscosity of water which increases the diffusion rate of water through the membrane and thus, its water permeability coefficient. The same would be expected to occur in the FO process as well.

Temperature will also affect both ECP and ICP. An increased diffusion coefficient for the aqueous NaCl will increase the mass transfer coefficient, reducing the impact of the ECP modulus (making it closer to a value of one). The effect is similar for the ICP modulus, where an increased diffusion coefficient reduces solute resistivity. However, since both the ECP and ICP moduli are exponential functions of the permeate water flux as well, the temperature effect on these phenomena will be lessened, as an increase in the water permeability coefficient of the membrane

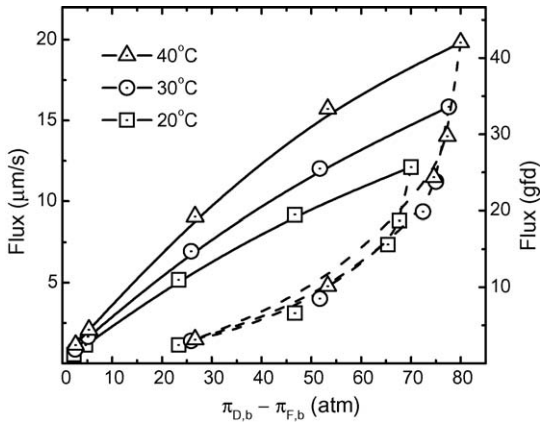

Fig. 3. Flux data plotted against the osmotic pressure difference between the bulk feed and draw solutions at 20, 30, and 40 °C. The draw solution is against the active layer and the feed solution is against the support layer. Experimental procedure described in Section 2.4 and Fig. 1. Experimental conditions: crossflow rate of both feed and draw solution is 45.8 cm/s, indicated temperatures apply to both feed and draw solution. Note that a water flux of 10 μm/s corresponds to 21.2 gal ft^{-2} d^{-1} (gfd) or 36.01 m^{-2} h^{-1}.

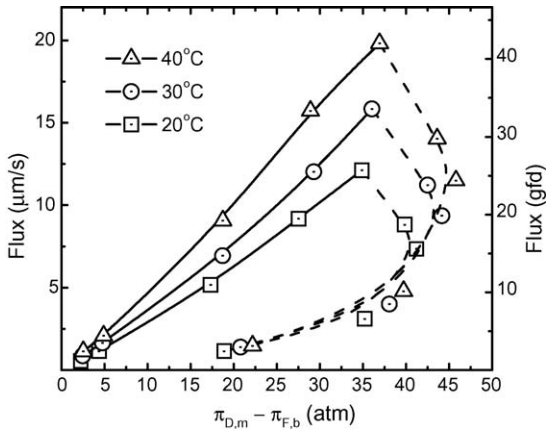

Fig. 4. Flux and driving force data (from Fig. 3) after correction for external concentration polarization (ECP) along the active layer (permeate side). The draw solution is against the active layer and the feed solution is against the support layer. Experimental protocol described in Section 2.4 and Fig. 1. Experimental conditions: crossflow rate of both feed and draw solution is 45.8 cm/s, indicated temperatures apply to both feed and draw solution. Note that a water flux of 10 μm/s corresponds to 21.2 gal ft^{-2} d^{-1} (gfd) or 36.01 m^{-2} h^{-1}.

will increase flux. The data below show our results for both orientations of the membrane for each temperature.

4.1.1. Draw solution against the active layer

Fig. 3 presents flux data for FO runs in the PRO mode. Flux is presented as a function of the osmotic pressure difference between the bulk feed and draw NaCl solutions. The data follow the protocol described in Fig. 1. Notice the significant increase in flux with an increase in solution temperature, as hypothesized above, for data representing flux in the absence of concentrative ICP with DI water as feed (solid line). In the presence of ICP (dashed line), the data suggest that temperature plays a negligible role.

First, let us look at the solid lines in Fig. 3. A proportional increase in flux would be expected with an increase in the effective osmotic pressure difference between the draw and feed solutions. Since no NaCl is present in the feed solution, the nonlinear flux behavior can be attributed entirely to dilutive ECP on the permeate side [7]. We would expect dilutive ECP to be significant given the high water fluxes attained during these tests, particularly at the higher osmotic pressure difference and temperature.

As soon as NaCl is added to the deionized feed solution, the flux drops precipitously, even for low bulk feed concentrations. This is due to the development of concentrative ICP within the porous support layer. This hysteresis effect indicates the significant impact concentrative ICP has on water flux, even at low bulk feed concentrations. Even these low bulk feed concentrations can cause severe ICP given the high water fluxes.

To isolate the effect of dilutive ECP from the concentrative ICP, where the two phenomena are coupled, we can use the film theory as described above in Section 3.3. The purpose of doing so is to verify that the water permeability coefficient obtained from the FO experiments is equal to the pure water hydraulic permeability as well as to compare the severity of the ECP and the ICP at the given temperatures. Fig. 4 shows the data from Fig. 3 corrected for dilutive ECP on the active layer (permeate side). In this step, we replace the bulk draw solution osmotic pressure, $\pi_{D,b}$, with the calculated draw solution osmotic pressure at the surface of the membrane active layer, $\pi_{D,m}$. Again, we assume that ECP does not occur on the support layer.

The data indicate two very important flux behaviors. First, for a DI water feed, as the draw solution concentration against the active layer is increased, the flux increases linearly with increased osmotic pressure driving force based on the membrane surface concentration of the draw solution. The slopes of these lines match the pure water permeability (determined by RO) of the membrane at the indicated temperatures. This matching of the pure water permeability data to the osmotic flux data suggests that our assumption about insignificant salt passage from the draw to the feed is reasonable. If there was significant salt passage from the draw solution, then these lines would be curved due to the presence of concentrative ICP. It is also observed that the effective driving force in Fig. 4 is significantly lower than the driving force indicated in Fig. 3. Dilutive ECP causes this significant decrease in driving force for several reasons. First, the cell channel is rather deep (3 mm) and the Reynolds number is relatively low ($Re \approx 1000$). These hydrodynamic conditions lead to a dilutive ECP modulus which is significantly less than one. Second, we must remember that the ECP is acting on the draw solution, which is very concentrated. Pure water permeating the membrane has a considerable dilutive effect on these concentrated draw solutions. The data also indicate that ECP is also very severe at higher temperatures, even in the presence of higher diffusion coefficients. As mentioned earlier, the increased water flux due to higher water permeability counteracts the effect of the increased diffusion coefficient.

Fig. 4 shows that higher temperatures do indeed result in a reduced severity of ICP. In Fig. 3, one could not distinguish the flux behavior between the 20, 30, and 40 °C tests in the presence of dilutive ECP coupled with concentrative ICP. Once the effect of dilutive ECP is accounted for, as in Fig. 4, it is clear

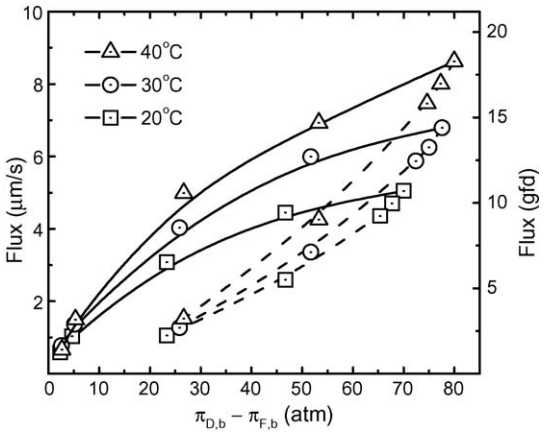

Fig. 5. Flux data plotted against the osmotic pressure difference between the bulk feed and draw solutions at 20, 30, and 40 °C. The draw solution is against the support layer and the feed solution is against the active layer. Experimental procedure described in Section 2.4 and Fig. 1. Experimental conditions: crossflow rate of both feed and draw solution of 45.8 cm/s, indicated temperatures apply to both feed and draw solution. Note that a water flux of 10 μm/s corresponds to 21.2 gal ft^{-2} d^{-1} (gfd) or 36.01 m^{-2} h^{-1}.

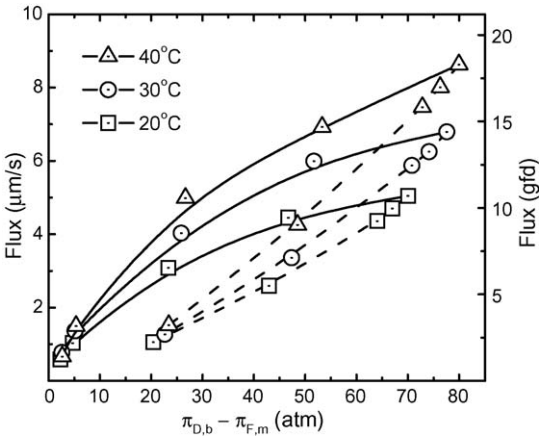

Fig. 6. Flux and driving force data from Fig. 5 after correction for external concentration polarization (ECP) along the active layer (feed side). The draw solution is against the support layer and the feed solution is against the active layer. Experimental procedure described in Section 2.4 and Fig. 1. Experimental conditions: crossflow rate of both feed and draw solution is 45.8 cm/s. Note that a water flux of 10 μm/s corresponds to 21.2 gal ft^{-2} d^{-1} (gfd) or 36.01 m^{-2} h^{-1}.

that less concentrative ICP exists at higher temperatures, at least for lower feed concentrations. Another interesting result is that the effective driving force *increases* upon the addition of salt to the feed (data connected with dashed lines), even though flux is decreasing. The sharp decrease in flux is due to concentrative ICP; yet a decreased flux also reduces the extent of dilutive ECP, which is very severe at the high draw solution concentration and high flux prior to the addition of salt to the feed. The negative contribution of concentrative ICP to the osmotic driving force at low bulk feed concentrations is masked by the marked reduction in dilutive ECP modulus at lower fluxes. Flux reduction due to ICP becomes dominant after the feed concentration surpasses 0.5 M NaCl, since further reduction in water flux has only marginal effects on the dilutive ECP and bulk feed concentrations are high enough to create severe concentrative ICP within the porous support, even at lower fluxes.

4.1.2. Draw solution against the support layer

Flux data were taken under the same system conditions as described in Section 4.1.1, except that the membrane was oriented in the FO mode. The resulting water flux behavior is presented in Fig. 5. The solid lines now indicate flux under the influence of dilutive ICP in the absence of concentrative ECP (because the feed is DI water). The non-linear flux behavior with increasing draw solution concentrations is attributed to this dilutive ICP. Similar flux behavior was observed in our previous studies on FO [6,7]. The ICP is also responsible for the significantly lower water flux rates when compared to Fig. 3. Increasing the temperature resulted in increased water flux, though overall, the flux rates were still quite low in comparison to the data above for the PRO mode.

Upon addition of salt to the feed solution, flux decreases due to what was thought to be a combined effect of decreased osmotic pressure driving force and concentrative ECP. This was not the case, however, as illustrated in Fig. 6. The driving force in this figure is adjusted to account for the effects of concentrative ECP (similar to Fig. 4). Note that accounting for concentrative ECP only changes the data connected by dashed lines since the data connected by solid lines indicate a deionized water feed and therefore, are not affected by ECP. The change in the affected data points is negligible, however, because of two conditions. First, the permeate fluxes are relatively low, keeping the ECP modulus relatively close to a value of one when compared to those presented in Figs. 3 and 4. Second, concentrative ECP reduces effective driving force to a lesser extent due to relatively low feed concentrations when compared to the draw solution. The highest fluxes occur with the lowest feed concentrations and hence ECP has only a minor effect on effective driving forces. As feed concentrations increase, lower water fluxes yield an ECP modulus closer to one, further mitigating the negative contribution to the overall driving force. Thus the decrease in water flux due to the addition of NaCl to the feed is due primarily to the decreased bulk osmotic pressure difference.

It is also important to note the hysteresis effect associated with the data in Fig. 6. It would seem contradictory to observe a change in flux behavior as a function of driving force with the addition of a salt against the active layer of the membrane, because the addition of this salt does not create additional ICP. If anything, the lower flux rates caused by the increased feed concentration should decrease the severity of the dilutive ICP. This result is attributed, rather, to the increased severity of dilutive ICP at a higher draw solution concentration, as suggested in McCutcheon et al. [7]. Higher draw solution concentrations produce less flux at a given bulk osmotic pressure difference due to an increased degree of dilution within the porous support. The dotted line represents data using the highest draw solution concentration at 1.5 M NaCl. Tests with the same effective osmotic driving forces with a deionized water feed, represented by the solid line, utilized a lower draw solution concentration resulting in a higher flux at a given bulk osmotic pressure difference due to a lesser ICP effect.

4.2. Predicted flux behavior

Modeling can help predict how flux performance will change with varying system conditions or membrane structure and therefore, help to optimize performance without time consuming or expensive experimentation. The models used here were presented in Sections 3.2 and 3.3. Previous studies [8,19] ignored the presence of ECP, which may have been a valid assumption because water fluxes were very low. In the case of the data presented above, water flux rates are far too high to ignore the presence of ECP, particularly in the PRO mode.

To solve for the permeate flux at a given bulk osmotic pressure difference, Eqs. (12) and (16) require that we know the water permeability coefficient, A, the mass transfer coefficient, k, and the solute resistivity for diffusion, K. The water permeability coefficient is determined by reverse osmosis testing at the appropriate temperature. The mass transfer coefficient can be calculated as described in Section 3.1. The solute resistivity, defined in Eq. (9), is a bit more complicated to determine. While the diffusion coefficient of aqueous NaCl is available in literature, the thickness, tortuosity, and porosity of the porous support for a particular membrane cannot be determined experimentally with great accuracy. However, since these three structural characteristics do not change for membranes that are mechanically and chemically stable under the chosen experimental conditions, the term $KD = t\tau/\varepsilon$ will be constant for a given membrane. To verify that this model predicts flux accurately for our FO membrane, we first determine the value of $t\tau/\varepsilon$ for this membrane. The experimental data taken at 20 °C was used to determine $t\tau/\varepsilon$ as summarized in Table 1.

It is interesting to note that the average $t\tau/\varepsilon$ value for the PRO (i.e., feed against the support layer) and FO (i.e., feed against the active layer) modes differ from one another. The small difference may arise from varying diffusion coefficient of the NaCl within the porous support due to varying NaCl concentration. The difference may also be due to the asymmetry of the support layer itself. The model assumes a homogenous support structure and asymmetry may cause different diffusion behavior depending on the direction of the water flux and dissolved ion transport. For modeling water flux in the PRO and FO modes, the corresponding average values of $t\tau/\varepsilon$ were used in Eqs. (12) and (16), respectively. All other parameters in these equations are defined under specified solution concentrations, hydrodynamic conditions, and temperatures.

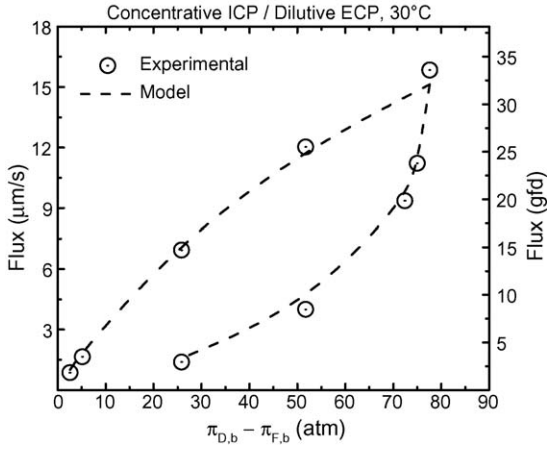

Fig. 7. Flux data plotted against the osmotic pressure differences between the bulk feed and draw solutions at 30 °C. Circles indicate experimental data from Fig. 3, dashed line indicates model as given in Eq. (12). Model prediction is based on a $t\tau/\varepsilon$ value of 2.98×10^{-4} m and a diffusion coefficient of 1.73×10^{-9} m^2/s. Experimental conditions: draw solution against the active layer, feed solution against the support layer (concentrative ICP, dilutive ECP), crossflow rate and temperature of both feed and draw solution is 45.8 cm/s and 30 °C, respectively. Note that a water flux of 10 μm/s corresponds to 21.2 gal ft^{-2} d^{-1} (gfd) or 36.01 m^{-2} h^{-1}.

4.2.1. Draw solution against the active layer

Fig. 7 shows the 30 °C data given in Fig. 3 (open symbols) compared to predictions (dashed lines) based on Eq. (12). The

Table 1
Data for 20 °C osmosis runs in the FO and PRO mode. Eqs. (8) and (13), respectively, were used to determine K values [18], from which $t\tau/\varepsilon$ was calculated using a diffusivity of 1.33×10^{-9} m^2/s for NaCl [20]

Active layer		Backing layer		Flux (μm/s) (gfd)	K (10^5 s/m)	$t\tau/\varepsilon$ (10^{-4} m)
Concentration (M)	Osmotic pressure[a] (atm) (psi)	Concentration (M)	Osmotic pressure (atm) (psi)			
Concentrative ICP, dilutive ECP (PRO mode)						
1.50	42.17 (619.53)	0.05	2.33 (34.3)	8.82 (18.69)	2.02	2.69
1.50	45.88 (673.91)	0.10	4.67 (68.6)	7.35 (15.59)	2.12	2.82
1.50	58.56 (860.32)	0.50	23.35 (343.0)	3.11 (6.60)	2.36	3.13
1.50	65.59 (963.52)	1.00	46.70 (685.9)	1.14 (2.42)	2.47	3.29
Average					2.24	2.98
Dilutive ICP, concentrative ECP (FO mode)						
0.00	0.00 (0.00)	1.50	70.04 (1028.9)	5.05 (10.70)	2.83	3.76
0.05	3.06 (44.96)	1.50	70.04 (1028.9)	4.70 (9.97)	2.80	3.73
0.10	6.00 (88.15)	1.50	70.04 (1028.9)	4.36 (9.24)	2.81	3.74
0.50	27.11 (398.23)	1.50	70.04 (1028.9)	2.59 (5.50)	2.56	3.41
1.00	49.63 (729.06)	1.50	70.04 (1028.9)	1.06 (2.25)	2.52	3.35
Average					2.70	3.60

[a] Osmotic pressure at membrane surface, adjusted for external CP.

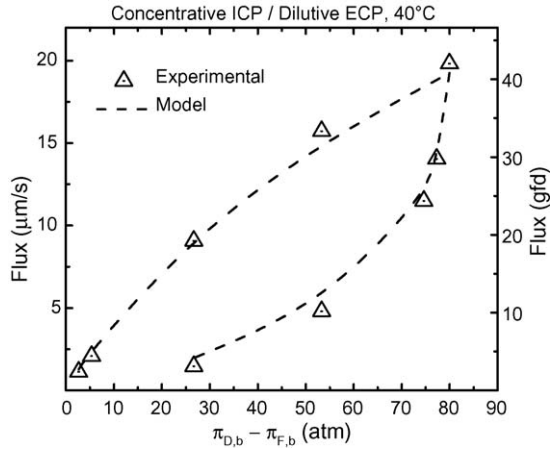

Fig. 8. Flux data plotted against the osmotic pressure differences between the bulk feed and draw solutions at 40 °C. Triangles indicate experimental data from Fig. 3, dashed line indicates model as given in Eq. (12). Model prediction is based on a $t\tau/\varepsilon$ value of 2.98×10^{-4} m and a diffusion coefficient of 2.12×10^{-9} m^2/s. Experimental conditions: draw solution against the active layer, feed solution against the backing layer (concentrative ICP, dilutive ECP), crossflow rate and temperature of both feed and draw solution is 45.8 cm/s and 40 °C, respectively. Note that a water flux of 10 μm/s corresponds to 21.2 gal ft^{-2} d^{-1} (gfd) or 36.01 m^{-2} h^{-1}.

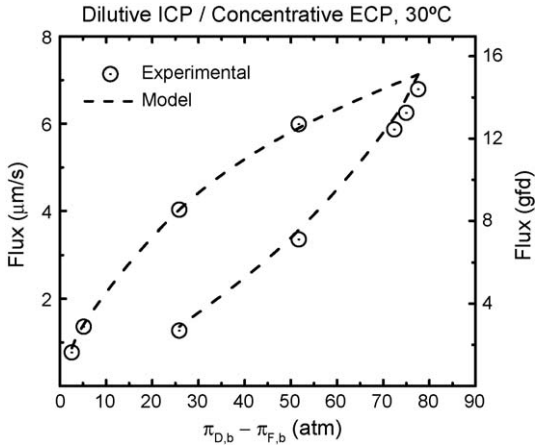

Fig. 9. Flux data plotted against the osmotic pressure differences between the bulk feed and draw solutions at 30 °C. Circles indicate experimental data from Fig. 5, dashed line indicates model as given in Eq. (16). Model prediction is based on a $t\tau/\varepsilon$ value of 3.60×10^{-4} m and a diffusion coefficient of 1.73×10^{-9} m^2/s. Experimental conditions: draw solution against the support layer, feed solution against the active layer (dilutive ICP, concentrative ECP), crossflow rate and temperature of both feed and draw solution is 45.8 cm/s and 30 °C, respectively. Note that a water flux of 10 μm/s corresponds to 21.2 gal ft^{-2} d^{-1} (gfd) or 36.01 m^{-2} h^{-1}.

average value of $t\tau/\varepsilon$ given in Table 1 (i.e., 2.98×10^{-4} s/m) and a diffusion coefficient of 1.73×10^{-9} m^2/s [20] were used to calculate the K value at this temperature. The temperature effect on the mass transfer coefficient has also been taken into account (for viscosity, diffusion coefficient, and density). The same is true for Fig. 8, where the points indicate experimental data given in Fig. 3 for 40 °C tests and the dashed line indicates the model prediction, this time with all parameters calculated taking into account the temperature condition of 40 °C (diffusion coefficient of 2.12×10^{-9} m^2/s).

The model fits the experimental data very well for both temperatures. This indicates that the model can be used with this particular value of $t\tau/\varepsilon$ in the PRO mode to accurately predict flux under a variety of hydrodynamic or temperature conditions. It can be used for other membranes also, but the assumption that $B = 0$ must still be valid and new values of $t\tau/\varepsilon$ and A must be obtained using experimental data.

4.2.2. Draw solution against the backing layer

When the membrane is in the FO mode, we encounter a situation in which dilutive ICP is coupled with concentrative ECP. Again, we can use the averaged $t\tau/\varepsilon$ values (FO mode) taken at 20 °C to predict flux for the dilutive ICP coupled with concentrative ECP, as shown in Eq. (16). The results of the model shown with the experimental data taken at 30 °C (from Fig. 5) are shown in Fig. 9. The 40 °C data from Fig. 5 and the corresponding model are shown in Fig. 10.

Again, excellent agreement between the experimental data and the model show that the model is accurate for our FO membrane at the given hydrodynamic conditions. With the validity of the model proven against experimental data for both orientations (i.e., PRO and FO modes), we can use it as a reliable stand-alone predictor for flux based on changing membrane or system characteristics.

4.3. Improving water flux in forward osmosis

Previous studies on PRO and FO processes have concluded that the primary obstacle to the development of an economic osmotic process is the presence of internal concentration polarization. Reducing the prevalence of this phenomenon will improve the performance, and therefore the economic viability, of the FO and PRO osmotic processes. The data presented here have shown that changing the system conditions, such as increasing temperature, has improved membrane flux

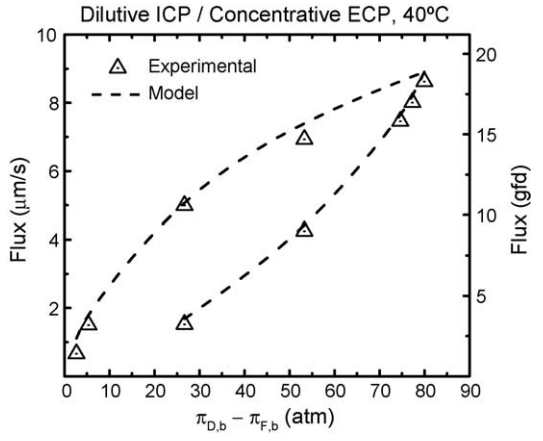

Fig. 10. Flux data plotted against the osmotic pressure differences between the bulk feed and draw solutions at 40 °C. Triangles indicate experimental data from Fig. 5, dashed line indicates model as given in Eq. (16). Model prediction is based on a $t\tau/\varepsilon$ value of 3.60×10^{-4} m and a diffusion coefficient of 2.12×10^{-9} m^2/s. Experimental conditions: draw solution against the support layer, feed solution against the active layer (dilutive ICP, concentrative ECP), crossflow rate and temperature of both feed and draw solution is 45.8 cm/s and 40 °C, respectively. Note that a water flux of 10 μm/s corresponds to 21.2 gal ft^{-2} d^{-1} (gfd) or 36.01 m^{-2} h^{-1}.

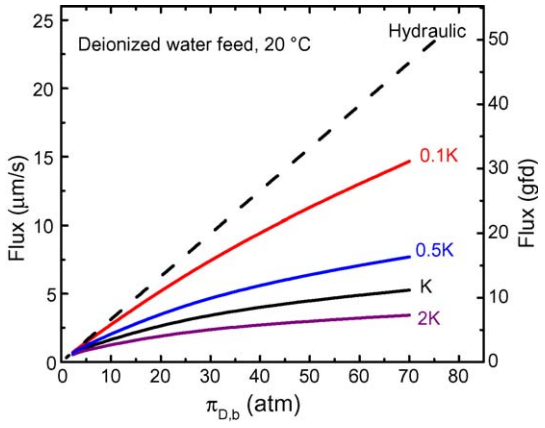

Fig. 11. Predicted flux in the FO mode based on model given in Eq. (16). A K value of 2.70×10^5 s/m is used for the line marked "K" (given in Table 1 for the CA membrane). K is then changed by the indicated factor to show the effect on water flux performance. The draw solution has a maximum concentration of 1.5 M NaCl and is against the support layer (dilutive ICP). The feed is assumed to be deionized water and is against the active layer (no concentrative ECP). The dotted line indicates the hydraulic permeability of the membrane using pure water.

performance in the absence of ICP. However, in the presence of ICP, these improvements are marginalized by self-limiting flux behavior. Our ability to reduce the prevalence of ICP is limited when we only attempt to control the system conditions external to the membrane.

The only way to markedly reduce the prevalence of ICP is to limit flux or to reduce the solute resistance to diffusion, K. In PRO, flux may be kept low intentionally by pressurizing the permeate side. This is not the case in FO, however, where limiting flux reduces the rate at which product water is obtained. So in FO, the only option is to reduce the value of K. This can be done external to the membrane only by increasing the diffusion coefficient, a feat only possible by increasing temperature or changing the draw solute. Temperature dependency on flux was shown above and the modest effect on ICP can be seen in Figs. 5 and 6. Changing the draw solute is rarely an option since the solute recovery step is critical in determining the economics of the FO process. The only other option is to tailor the membrane for more optimal osmotic performance by making the membrane porous support layer more porous or less thick (tortuosity is more difficult to control). The reduction of K can be accomplished by any combination of these modifications.

We can determine the effect of changing K by numerically solving Eq. (12) or (16), depending on the membrane orientation and system conditions, for different values of K, using our FO membrane as a basis. Fig. 11 shows a simplified case in the FO mode based on the exact flow and temperature conditions as described earlier in the paper with our FO membrane. The solid line labeled K indicates the predicted flux for 20 °C over a range of NaCl draw solution concentrations for our FO membrane with a deionized water feed. When K is changed by the indicated factor, the flux profile changes. As anticipated, lower K values result in higher predicted fluxes for identical bulk osmotic driving forces. More pronounced is the change in the required draw solution osmotic pressure for a given flux. For example, for a desired flux of 10 gfd (4.72 μm/s), a decrease in K by only a factor of 2 from our current FO membrane leads to reduction of required draw solution osmotic pressure from 45 to 20 atm, more than halving the draw concentration. These differences become more pronounced at higher fluxes. This fact has serious ramifications with regard to the draw solute recovery process since lower draw solution concentrations will require less energy to separate.

The flux behavior in the presence of dilutive ICP becomes more ideal the lower K becomes. Ideal flux behavior is given by the dashed line which represents the pure water permeability data as determined from RO. The model, however, can only be used assuming that no ECP takes place on the support layer side of the membrane. Thus, as K approaches zero (i.e., no porous support layer), this assumption is no longer valid, especially for high permeate water fluxes and more concentrated draw solutions.

5. Concluding remarks

In this investigation, the coupled effects of internal and external concentration polarization on permeate flux were elucidated and discussed for forward osmosis across a commercially available forward osmosis membrane. This membrane, which is asymmetric in nature, was found to exhibit flux reductions due to severe internal concentration polarization in both the PRO and FO modes. External concentration polarization was found to negatively impact osmotic driving force when the membrane was used in the PRO mode, though its effect was relatively small in the FO mode. Increased temperature was found to improve flux performance, but increases were limited due to the severity of internal and external concentration polarization at higher fluxes. Flux models accounting for both internal and external concentration polarization in both the PRO and FO modes were presented and used to predict flux under specified experimental conditions. These models relied on the experimental determination of the solute's resistance to diffusion, K, which is a measure of a solute's ability to diffuse into and out of the membrane porous support layer. Data collected from forward osmosis tests were found to closely match model predictions. With the availability of a standalone model, it was determined that flux could be predicted accurately based on assumed changes in membrane structure. Modest changes in membrane structure, leading to a reduction in K, were found to significantly improve flux performance and reduce necessary osmotic driving forces in FO. Further studies exploring the coupling of ECP and ICP would help predict flux performance based on membrane characteristics and hydrodynamics. Optimization of these parameters would contribute to the design and fabrication of an improved membrane, tailored for the forward osmosis process.

Acknowledgements

The authors would like to acknowledge the Office of Naval Research, Award No. N00014-03-1-1004, for supporting this work. The authors also acknowledge Hydration Technologies for providing membranes.

References

[1] C.D. Moody, J.O. Kessler, Forward osmosis extractors, Desalination 18 (1976) 283–295.

[2] J.O. Kessler, C.D. Moody, Drinking-water from sea-water by forward osmosis, Desalination 18 (1976) 297–306.

[3] W.T. Hough, Solvent extraction into a comestible solute, US Patent 3,670,897, 1970.

[4] R.L. McGinnis, Osmotic desalination process, US patent 6,391,205 B1, 2002.

[5] R.L. McGinnis, Osmotic desalination process, US Pending PCT/US02/02740.

[6] J.R. McCutcheon, R.L. McGinnis, M. Elimelech, A novel ammonia-carbon dioxide forward (direct) osmosis desalination process, Desalination 174 (2005) 1–11.

[7] J.R. McCutcheon, R.L. McGinnis, M. Elimelech, Desalination by ammonia–carbon-dioxide forward osmosis: influence of draw and feed solution concentrations on process performance, J. Membr. Sci. 278 (2006) 114–123.

[8] K.L. Lee, R.W. Baker, H.K. Lonsdale, Membranes for power-generation by pressure-retarded osmosis, J. Membr. Sci. 8 (1981) 141–171.

[9] S. Loeb, F. Vanhessen, D. Shahaf, Production of energy from concentrated brines by pressure-retarded osmosis 2: experimental results and projected energy costs, J. Membr. Sci. 1 (1976) 249–269.

[10] S. Loeb, Energy production at the dead sea by pressure-retarded osmosis: challenge or chimera? Desalination 120 (1998) 247–262.

[11] S. Loeb, Large-scale power production by pressure-retarded osmosis, using river water and sea water passing through spiral modules, Desalination 143 (2002) 115–122.

[12] S. Loeb, One hundred and thirty benign and renewable megawatts from great salt lake? The possibilities of hydroelectric power by pressure-retarded osmosis with spiral module membranes, Desalination 141 (2001) 85–91.

[13] R.W. Baker, Membrane Technology and Applications, Wiley, West Sussex, 2004.

[14] S.S. Sablani, M.F.A. Goosen, R. Al-Belushi, M. Wilf, Concentration polarization in ultrafiltration and reverse osmosis: a critical review, Desalination 141 (2001) 269–289.

[15] M. Elimelech, S. Bhattacharjee, A novel approach for modeling concentration polarization in crossflow membrane filtration based on the equivalence of osmotic pressure model and filtration theory, J. Membr. Sci. 145 (1998) 223–241.

[16] G.D. Mehta, S. Loeb, Internal polarization in the porous substructure of a semipermeable membrane under pressure-retarded osmosis, J. Membr. Sci. 4 (1978) 261–265.

[17] M. Mulder, Basic Principles of Membrane Technology, Kluwer Academic, Dordrecht, 1996.

[18] G.T. Gray, J.R. McCutcheon, M. Elimelech, Internal concentration polarization in forward osmosis: role of membrane orientation, Desalination 197 (2006) 1–8.

[19] S. Loeb, L. Titelman, E. Korngold, J. Freiman, Effect of porous support fabric on osmosis through a Loeb-Sourirajan type asymmetric membrane, J. Membr. Sci. 129 (1997) 243–249.

[20] V.M.M. Lobo, Mutual diffusion-coefficients in aqueous-electrolyte solutions (technical report), Pure Appl. Chem. 65 (1993) 2614–2640.